Short Communication

Skin Pharmacology and Physiology

Skin Pharmacol Physiol 2012;25:93–99
DOI: 10.1159/000335257

Received: April 19, 2011
Accepted after revision: November 17, 2011
Published online: February 1, 2012

Coriandrum sativum L. Protects Human Keratinocytes from Oxidative Stress by Regulating Oxidative Defense Systems

G. Park[a] H.G. Kim[b] Y.O. Kim[c] S.H. Park[d] S.Y. Kim[d] M.S. Oh[a, b]

[a]Department of Life and Nanopharmaceutical Science and Kyung Hee East-West Pharmaceutical Research Institute, and [b]Department of Oriental Pharmaceutical Science, College of Pharmacy, Kyung Hee University, Seoul, [c]Department of Herbal Crop Research, National Institute of Horticultural and Herbal Science, Rural Development Administration, Bisan-ri, and [d]Department of Medical Science, Graduate School of East-West Medical Science, Kyung Hee University, Yongin-si, Republic of Korea

Key Words

Coriandrum sativum L. · Keratinocyte · Antioxidative · Nuclear factor erythroid-derived 2-related factor 2 · Oxidative defense enzymes

Abstract

Background: Oxidative radicals are major environmental causes of human skin damage. Oxidative defense factors, including nuclear factor erythroid-derived 2-related factor 2 (Nrf2), are centrally involved in repairing skin cells or protecting them from oxidative damage. *Coriandrum sativum* L. (coriander; CS) is a commonly consumed food and a traditional phytomedicine in Asia and Europe. In this study, we examined the protective effects of a standardized CS leaf extract against oxidative stress in human HaCaT keratinocytes. ***Methods and Results:*** CS significantly and dose-dependently protected cells against reduced cell viability caused by H_2O_2-induced damage, as assessed using the 3-(4,5-dimethylthiazol-2-yl)-2,5-diphenyltetrazolium bromide assay. Other assays demonstrated that CS protected HaCaT cells by increasing the levels of glutathione and activities of oxidative defense enzymes, such as superoxide dismutase and catalase. Moreover, it increased the expression of activated Nrf2, which plays a crucial role in protecting skin cells against oxidative stress. ***Conclusion:*** These results suggest that CS protects human keratinocytes from H_2O_2-induced oxidative stress through antioxidant effects.

Introduction

The skin, the largest organ of the human body, is constantly exposed to pro-oxidant environmental stresses, such as ultraviolet (UV) radiation [1, 2]. Chronic exposure of the skin to pro-oxidants results in the development of oxidative damage, leading to several skin disorders, including hyperpigmentation, immunosuppression, inflammation and premature aging of the skin [2]. H_2O_2 is produced when cells are exposed to extracellular stimuli, and it is easily converted into radicals, such as superoxide anion and hydroxyl radicals, which damage many cellular components [3, 4]. Radical production is eliminated by oxidative defense enzymes, such as superoxide dismutase (SOD), catalase (CAT) and glutathione

KARGER

Fax +41 61 306 12 34
E-Mail karger@karger.ch
www.karger.com

1660–5527/12/0252–0093$38.00/0

Accessible online at:
www.karger.com/spp

M.S. Oh, OMD, PhD
Department of Life and Nanopharmaceutical Science
College of Pharmacy, Kyung Hee University
Hoegi-dong, Dongdaemun-gu, Seoul 130-701 (Korea)
Tel. +82 2 961 9436, E-Mail msohok@khu.ac.kr

(GSH). SOD catalyzes the dismutation of $\cdot O_2^-$ into O_2 (oxygen molecule) and H_2O_2, and CAT and GSH breaks H_2O_2 down into O_2 and H_2O. The combination of SOD, CAT and GSH scavenges radicals initiated by $\cdot O_2^-$ completely.

Recently, the transcription factor nuclear factor erythroid-derived 2-related factor 2 (Nrf2) was reported to play a key role in the regulation of oxidative stress response systems in the skin [5, 6]. In an unstressed state, Nrf2 is anchored in the cytoplasm by specific inhibitors, such as kelch-like ECH-associated protein 1 (Keap1) [6]. In the presence of stimulants, such as oxidants and UV radiation, Keap1 dissociates from Nrf2, allowing it to accumulate in the nucleus, where it binds to antioxidant response elements in the enhancers of target genes [6–9]. Nrf2 upregulates a set of antioxidants, including GSH, quione 1 and heme oxygenase 1, thereby protecting keratinocytes and fibroblasts in the skin from the ravages of oxidative stress [6, 8, 10].

Coriandrum sativum L. (coriander; CS), an annual herb that belongs to the carrot family (Umbelliferae), is cultivated extensively in Europe and Asia [11]. The leaves of CS are commonly eaten as a food seasoning and the seeds are used as a spice. CS is also used to treat cough, dysentery, rheumatism and giddiness in traditional medicine [11, 12]. Previous studies reported that it has anti-inflammatory potential in UV erythema and antioxidant effects in rats fed a high-fat diet [13, 14]. Chemically, CS is known to contain large amounts of essential oils and fatty acids [15, 16]. It also contains well-known antioxidants, such as caffeic acid, ferulic acid, chlorogenic acid, linoleic acid and linolenic acid [17].

In this study, we evaluated the effect of a CS leaf extract on H_2O_2-induced oxidative stress in human HaCaT keratinocytes. To investigate its protective effects, we measured cell viability using the 3-(4,5-dimethylthiazol-2-yl)-2,5-diphenyltetrazolium bromide (MTT) assay. Then, to identify the possible mechanisms involved, we measured reactive oxygen species (ROS) production, GSH levels, and the activities of SOD and CAT, and Nrf2 immunofluorescence.

Materials and Methods

Chemical

Dulbecco's modified Eagle's medium, fetal bovine serum and penicillin-streptomycin were purchased from Hyclone Laboratories Inc. (Logan, Utah, USA). MTT, dimethylsulfoxide, hydrogen peroxide, 2,7-dichlorodihydrofluorescein diacetate (DCFH-DA) and N-acetyl-L-cysteine (NAC) were purchased from Sigma-Aldrich (St. Louis, Mo., USA). SOD activity and GSH quantification kits were purchased from Dojindo Molecular Technologies (Kumamoto, Japan). The CAT activity kit was purchased from Molecular Probes Invitrogen (Cergy-Pintoise, France). Tetramethylethylenediamine, protein standards dual color, western view marker, protein assay, Tween-20, acrylamide, ammonium persulfate, skim milk, and ECL reagent were purchased from Bio-Rad Laboratories (Hercules, Calif., USA). A nuclear/cytosol fraction kit was purchased from BioVision (Mountain View, Calif., USA). Rabbit anti-Nrf2 was obtained from Abcam (Cambridge, UK). Anti-rabbit horseradish peroxidase secondary antibody was purchased from Assay Designs (Ann Arbor, Mich., USA). The other reagents used were of guaranteed or analytical grade.

Preparation of the CS Extract and Standardization

Fresh CS was obtained from a producing district (Incheon, Korea), and a voucher specimen (KHUOPS-CMH002) was deposited in the herbarium at the College of Pharmacy, Kyung Hee University (Seoul, Korea). Then, 100 g of CS leaves were ground with 1 liter of 70% ethanol in a blender for 5 min and this was stirred for 24 h at room temperature. Then, the extract was filtered, evaporated on a rotary vacuum evaporator and lyophilized (yield: 4.00%). The powder (CSE) was kept at 4°C before use. To achieve standardization, CSE was analyzed by gas chromatography. Samples were saponified at 95°C for 15 min with 2 ml of 0.5 N methanolic sodium hydroxide and methylated by addition of 2 ml of 14% boron trifluoride methanol. The mixture was incubated at 95°C for 1 h and then cooled to room temperature. After vigorous shaking with 1 ml of iso-octane, the mixture was allowed to settle for 5 min, and the upper layer was transferred to a clean tube and air-dried under nitrogen. The dried sample was resuspended in 200 μl of iso-octane. Fatty acid methyl esters were analyzed using an Agilent 6890N gas chromatograph equipped with a 100 m × 0.25 mm i.d. (0.20 μm film thickness) SP-2560 capillary column (Supelco, Milan, Italy). The injector and flame ionization detector temperature was 250°C. The oven temperature was held at 140°C for 1 min, and thereafter increased to 190°C at 3.5°C/min. After 35 min, the temperature was increased at 4°C/min to 230°C, held at 230°C for 10 min, and maintained at the final temperature of 240°C for 2 min. Peaks of interest were identified by comparison with the authentic standard mixture 37-Component FAME Mix (Supelco).

Cell Culture

HaCaT, a human keratinocyte cell line, was kindly donated by Prof. S.Y. Kim from Kyung Hee University, Korea. Cells were maintained in Dulbecco's modified Eagle's medium supplemented with 10% heat-inactivated fetal bovine serum, 100 U/ml penicillin, and 100 μg/ml streptomycin in a condition of 95% air and 5% CO_2 at 37°C. All experiments were carried out 12 h after the cells had been seeded on the 96-well plates and 24-well plates at densities of 1×10^4 and 2×10^4 cells/well, respectively.

Measuring Cell Viability

Cell viability was measured using the MTT assay. HaCaT cells were seeded on 96-well plates and treated with CSE at doses of 20–500 μg/ml for 7 h, or pretreated with CSE for 1 h and then stimulated with 1 mM H_2O_2 for an additional 6 h. The treated cells were incubated with 1 mg/ml MTT for 2 h. The MTT medium was aspirated carefully from the wells, and the formazan dye was elut-

ed using dimethylsulfoxide. The absorbance was measured using a spectrophotometer (Versamax microplate reader; Molecular Device, Sunnyvale, Calif., USA) at a wavelength of 570 nm and was expressed as a percent of the value for the control.

Measuring Intracellular ROS

Intracellular ROS generation was measured using DCFH-DA fluorescence dye. DCFH-DA enters cells passively and is converted into nonfluorescent DCFH, which reacts with ROS to form the fluorescent product DCF [18]. HaCaT cells were seeded on black 96-well plates or onto coverslips in 24-well plates and treated with CSE at doses of 100 and 500 μg/ml for 1 h. Then, they were stimulated with 1 mM H_2O_2 for an additional 30 min. The cells were incubated with 25 μM DCFH-DA for 30 min. The fluorescence intensity was determined at 485 nm excitation and 535 nm emission using a fluorescence microplate reader (SpectraMax Gemini EM, Molecular Device). Representative images were taken using a fluorescence microscope (Olympus Microscope System BX51; Olympus, Tokyo, Japan). For the assessment of intra- and interexperimental variability, 3 independent experiments were carried out in triplicate.

Measuring the SOD and CAT Activities

The SOD and CAT activities were detected using the SOD Assay Kit-WST (Dojindo) and Amplex Red Catalase Assay Kit (Invitrogen), respectively, according to the manufacturers' protocols. Briefly, cells were seeded on a 100-mm dish and treated with CSE at doses of 100 and 500 μg/ml for 1 h. Briefly, cells were seeded on a 100-mm dish and treated with CSE at doses of 100 and 500 μg/ml for 1 h. Then, they were stimulated with 1 mM H_2O_2 for an additional 6 h. The treated cells were lysed in 10 mM hydrochloric acid solution by freezing and thawing. Then, they were treated with 5% 5-sulfosalicylic acid. After centrifugation at 8,000 *g* for 10 min at 4°C, the supernatant was used to assess the SOD and CAT activity. The working solutions were added to the well containing the supernatant and incubated at 37°C for 20 min. The absorbance was measured using a spectrophotometer at a wavelength of 450 nm for SOD or the fluorescence intensity was measured using a fluorescence microplate reader at 530 nm excitation and 560 nm emission for CAT. Standard curves for the enzymatic activities of SOD and CAT were drawn using purified enzyme preparations. The enzyme-specific activities were expressed as units per milligram of protein. One unit of SOD activity was defined as the amount of enzyme that inhibits 50% of the WST-1 formazan per minute. One unit of CAT activity was defined as 1 μM of H_2O_2 consumed per minute.

Measuring the Total GSH Level

Total GSH levels were determined using a Total Glutathione Quantification Kit (Dojindo), according to the instruction manual [19]. Briefly, cells were seeded on a 100-mm dish and treated with CSE at doses of 100 and 500 μg/ml for 1 h. Then, they were stimulated with 1 mM H_2O_2 for an additional 6 h. The treated cells were lysed in 10 mM hydrochloric acid solution by freezing and thawing. Then, they were treated with 5% 5-sulfosalicylic acid. After centrifugation at 8,000 *g* for 10 min at 4°C, the supernatant was used to assess the GSH level. A coenzyme working solution, buffer solution and enzyme working solution were added to the wells containing the supernatant incubated at 37°C for 5 min. Then, GSH standard, sample and substrate working solutions were added for 10 min each. The absorbance was measured using a spectrophotometer at a wavelength of 405 nm, and the GSH concentrations were determined using a GSH standard calibration curve.

Measuring the Nrf2 Immunofluorescence

HaCaT cells were seeded onto coverslips in 24-well plates and treated for 1 h with CSE at doses of 100 and 500 μg/ml. Then, they were stimulated with 1 mM H_2O_2 for an additional 6 h. Next, the cells were fixed by incubation with 4% paraformaldehyde at room temperature for 30 min. Fixed HaCaT cells (on coverslips) were rinsed in PBS and then incubated overnight at 4°C with a rabbit anti-Nrf2 antibody (dilution 1:500). They were then incubated for 2 h with an Alexa Fluor 488-conjugated goat anti-rabbit IgG (dilution 1:500). Cells were finally washed in PBS and mounted using Vectashield Mounting Medium containing 4′,6-diamidino-2-phenylindole. Confocal immunofluorescent images were captured using an LSM 700 confocal microscope (Carl Zeiss, Thornwood, N.Y., USA), and the fluorescence intensity was measured using Axio Vision 4.4 (Carl Zeiss, Oberkochen, Germany). For the assessment of intraexperimental variability, 3 independent experiments were carried out in triplicate.

Western Blot Analysis

The cells were pretreated with CSE (100 and 500 μg/ml) for 1 h and were stimulated with 1 mM H_2O_2 for an additional 6 h for detection of Nrf2. The cells were lysed with protein extraction buffer for whole protein. Nuclear and cytosol fractions were lysed with the nuclear/cytosolic fraction kit according to the manufacturer's protocol. Cell lysates were separated on 15% sodium dodecyl sulfate polyacrylamide gel electrophoresis, and then separated proteins were electrophoretically transferred to a membrane. The membranes were incubated with 5% skim milk in TBST (25 mM Tris-Cl, 150 mM NaCl, 0.005% Tween-20) for 45 min. Then they were incubated with rabbit anti-Nrf2 (1:500 dilution) and mouse anti-β-actin (1:2,000 dilution) primary antibody overnight at 4°C, followed by incubation with horseradish peroxidase-conjugated anti-rabbit IgG for 1 h, respectively. Immunoreactive bands were detected using an ECL detection kit and visualized using the LAS-4000 mini system (Fujifilm Corp., Japan).

Statistical Analysis

All statistical parameters were calculated using Graphpad Prism 4.0 software. Values were expressed as the mean ± standard error of the mean (SEM). The results were analyzed by one-way analysis of variance. Differences with a p value <0.05 were considered statistically significant.

Results and Discussion

In this study, we evaluated the protective effects of CSE, analyzed by gas chromatography, against H_2O_2 stress in HaCaT cells by performing assays related with the oxidative defense system. First, to investigate the effect of CSE with regard to protecting against H_2O_2-induced cell toxicity, we measured cell viability using the

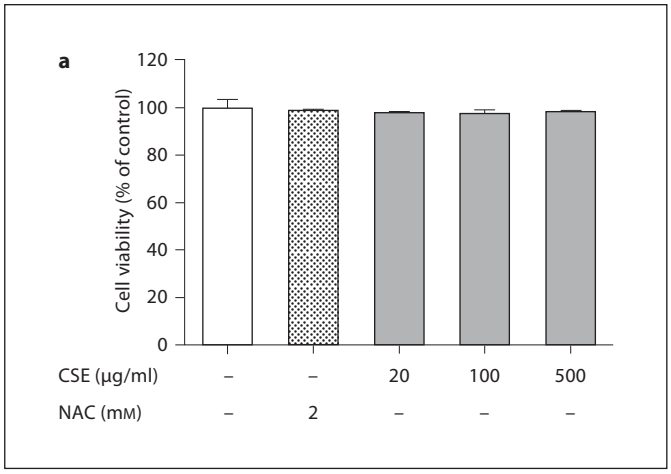

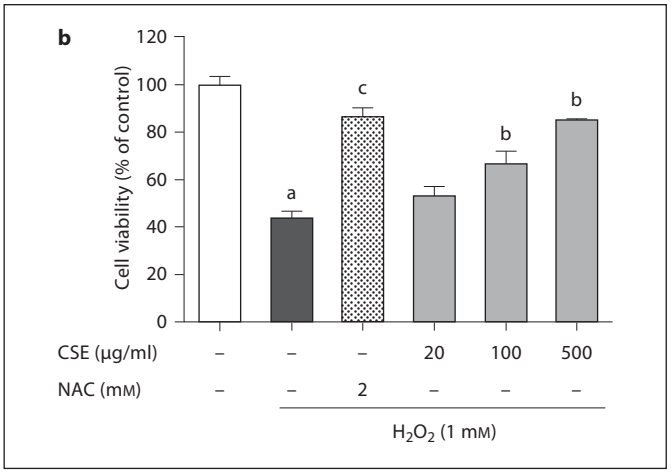

Fig. 1. Effects of CSE on H_2O_2-induced toxicity in HaCaT cells. After the cells had become confluent, they were treated with CSE or NAC for 1 h and incubated without (**a**) or with 1 mM H_2O_2 (**b**) for a further 6 h. Cell viabilities are expressed as a percentage of the controls. Values are given as the mean ± SEM. [a] $p < 0.001$, compared to the control group; [b] $p < 0.01$, [c] $p < 0.001$, compared to the H_2O_2-alone group.

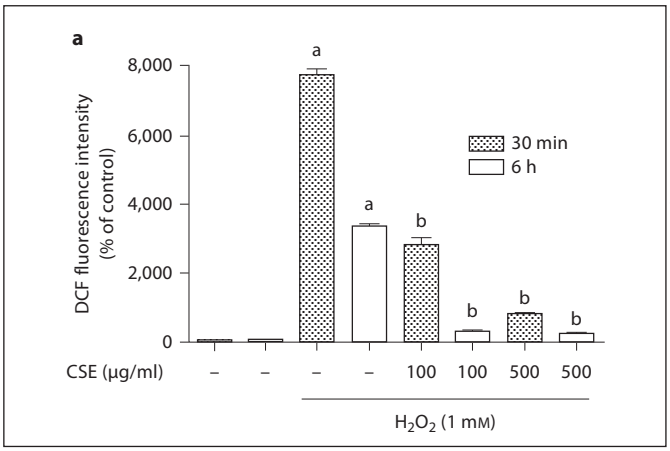

Color version available online

Fig. 2. Effect of CSE on the generation of ROS induced by H_2O_2 stress. The cells were treated with CSE for 1 h before stimulation with 1 mM H_2O_2. ROS generation was measured by the fluorescence intensity of DCF-DA after H_2O_2 stimulation for 30 min and 6 h (**a**). Representative pictures of this H_2O_2 stimulation for 30 min are shown (**b–e**): control group (**b**), H_2O_2-alone group (**c**), H_2O_2 + 100 μg/ml CSE group (**d**) and H_2O_2 + 500 μg/ml CSE group (**e**). Scale bar = 50 μm. Values are given as the mean ± SEM. [a] $p < 0.001$, compared to the corresponding control group; [b] $p < 0.001$, compared to the corresponding H_2O_2-alone group.

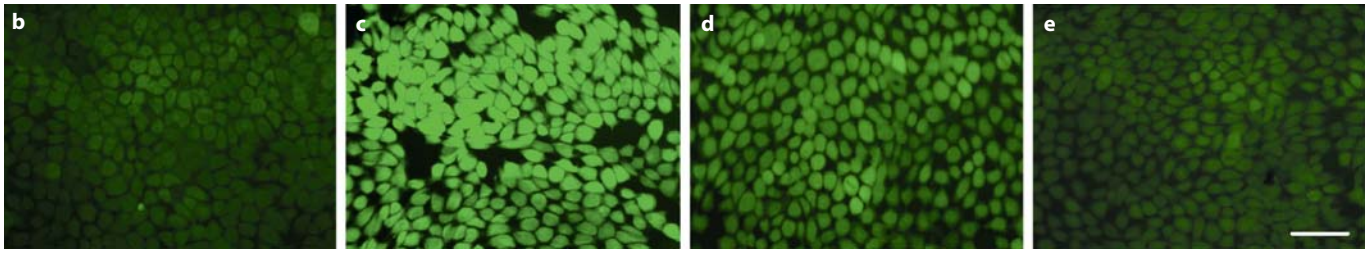

MTT assay. NAC, a dietary supplement commonly used as an antioxidative and skin-protecting agent, was used as a positive control [20]. The results showed that treatment with CSE at 20–500 μg/ml or NAC at 2 mM alone showed no effect on the cells (fig. 1a). Treatment with 1 mM H_2O_2 for an additional 6 h significantly reduced the cell viability to 43.87% compared to the control group, while pretreatment with CSE significantly attenuated it by 52.90–84.98% of the control at 20–500 μg/ml. CSE at 500 μg/ml showed a similar effect to 2 mM of NAC

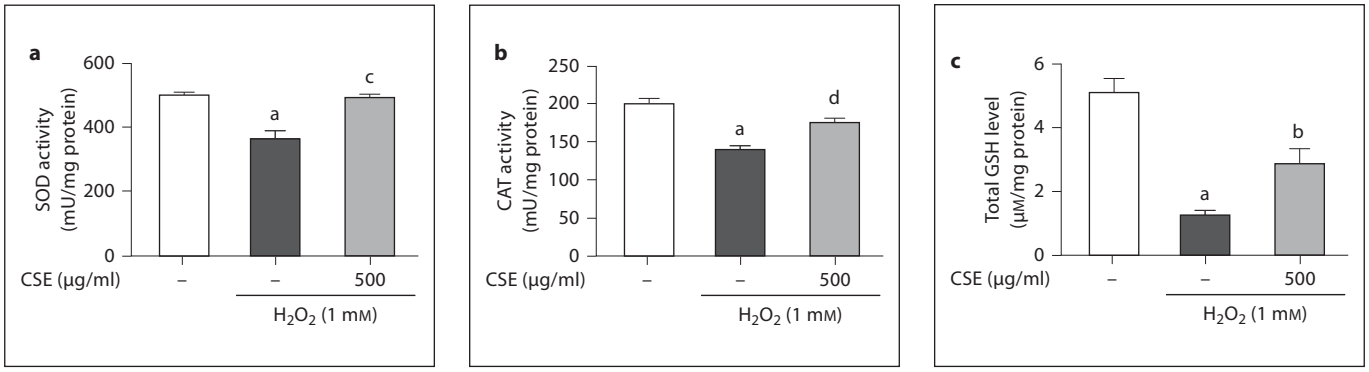

Fig. 3. Effect of CSE on H_2O_2-induced reduction in SOD and CAT activities and GSH levels in HaCaT cells. The cells were treated with CSE 500 μg/ml for 1 h, and then stimulated with 1 mM H_2O_2 for an additional 6 h. The activities of SOD (**a**) and CAT (**b**) and the level of GSH (**c**) were measured using each kit. The values are given as the mean ± SEM. [a] $p < 0.01$, compared to the control group; [b] $p < 0.05$, [c] $p < 0.01$, [d] $p < 0.001$, compared to the H_2O_2-alone group.

(fig. 1b). Then, to examine the effects of CSE on the H_2O_2-induced ROS generation, we assessed the intracellular ROS generation using DCFH-DA. ROS, potential inducers of apoptosis, cause intracellular oxidative damage in human keratinocytes [21]. In this study, treatment with 1 mM H_2O_2 for 30 min significantly increased ROS generation up to 77-fold compared with the control group, whereas treatment with 100 or 500 μg/ml CSE significantly reduced the ROS generation induced by H_2O_2 stress by 28- and 8-fold, respectively. Also, ROS generation was measured by the fluorescence intensity of DCF-DA after H_2O_2 stimulation for 6 h (fig. 2). From these results, CSE significantly reduced the ROS generation.

Next, to investigate the effect of CSE on the ROS-reducing enzyme system, we measured the activities of SOD and CAT which repair cells by reducing the damage by superoxide, the most common free radical, in the skin [2]. In this study, H_2O_2 caused significant SOD and CAT depletion (364.28 ± 24.66 and 140.70 ± 3.45 mU/mg protein, respectively), while CSE increased the SOD and CAT activities (494.93 ± 7.75 and 176.13 ± 4.19 mU/mg protein, respectively). Then, the effect of CSE on the GSH level was investigated, because GSH plays an important role in protecting against oxidative damage by catalyzing the reduction of oxidative stress, using GSH as the reducing substrate [22]. In this study, H_2O_2 induced significant GSH depletion (1.20 ± 0.12 μM/mg protein), while CSE increased the level (2.83 ± 0.66 μM/mg protein; fig. 3).

Finally, to investigate the possible regulation of Nrf2 by CSE, we measured nuclear expression of Nrf2 by immunofluorescence. To confirm the localization of Nrf2, we labeled the nuclei with 4′,6-diamidino-2-phenylindole. Treatment with 100 or 500 μg/ml CSE significantly increased Nrf2 expression, especially in the nucleus (294.44 ± 58.80 and 340.74 ± 80.35%, respectively, compared with control cells; fig. 4a). Figure 4 shows representative images indicating the marked increase in nuclear Nrf2 levels compared with untreated cells (fig. 4b). Also, to examine the effects of CSE on translocation of Nrf2 to nuclear protein under H_2O_2 stress, we assessed the Nrf2 nuclear protein level using Western blot analysis (fig. 4c).

Table 1. Analysis of CSE using gas chromatography

Component	Content mg/g
Undecanoic acid ($C_{11:0}$)	0.19
Lauric acid ($C_{12:0}$)	0.32
Tridecanoic acid ($C_{13:0}$)	0.51
Myristic acid ($C_{14:0}$)	0.13
Mytistoleic acid ($C_{14:1}$)	0.4
Pentadecanoic acid ($C_{15:0}$)	0.51
cis-10-Pentadecenoic acid ($C_{15:1}$)	0.9
Palmitic acid ($C_{16:0}$)	8.57
Palmitoleic acid ($C_{16:1}$)	0.65
Heptadecanoic acid ($C_{17:0}$)	0.18
Stearic acid ($C_{18:0}$)	0.98
Oleic acid ($C_{18:1}$, n–9c)	0.67
Linoleic acid ($C_{18:2}$, n–6c)	14.28
Linolenic acid ($C_{18:3}$, n–3)	17.91
cis-5,8,11,14,17-Eicosapentaenoic acid ($C_{20:5}$, n–3)	0.21
Behenic acid ($C_{22:0}$)	0.46
Total content	47.06

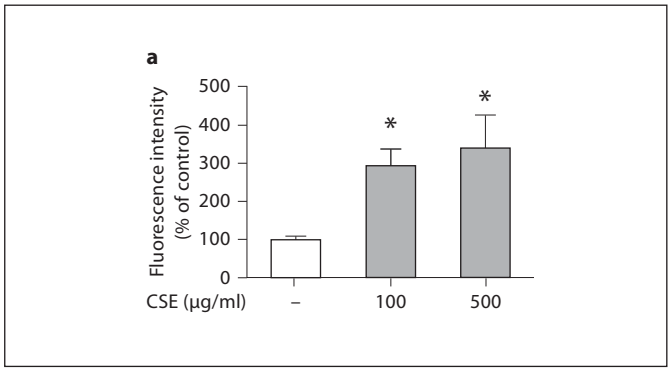

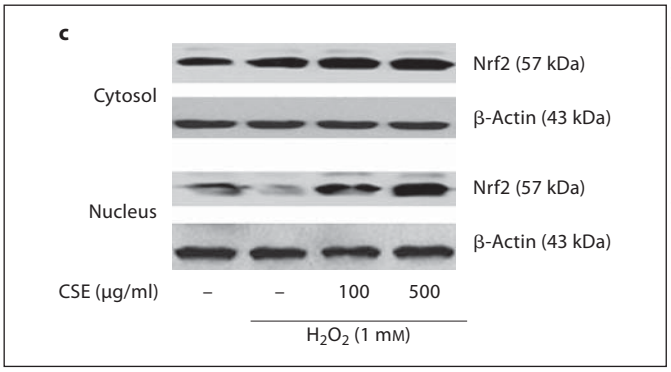

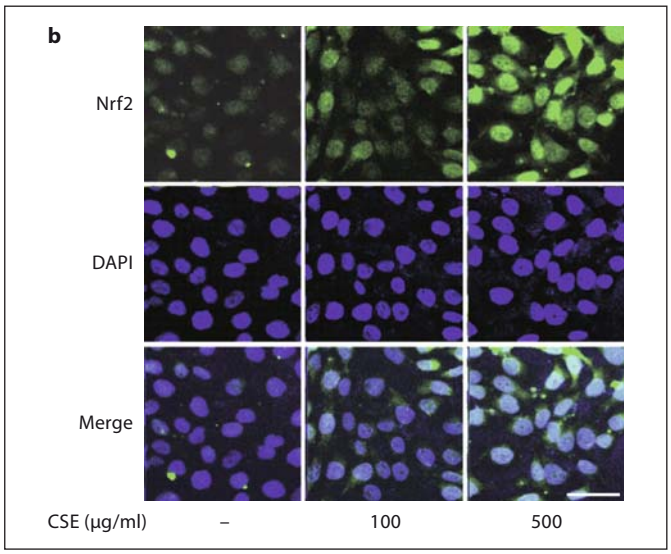

Color version available online

Fig. 4. Effect of CSE on Nrf2 expression in the nuclei of HaCaT cells. Nrf2 (green) was detected by immunofluorescence using an anti-Nrf2 antibody. Nuclei were visualized by 4′,6-diamidino-2-phenylindole (DAPI) staining (blue). **a** The fluorescence intensity due to Nrf2 translocation was measured. **b** Representative pictures. **c** Nrf2 nuclear protein levels. Scale bar = 25 μm. Values are given as the mean ± SEM. * $p < 0.05$, compared to the control group.

As shown in figure 4c, treatment with 1 mM H_2O_2 significantly decreased the Nrf2 nuclear protein level compared with the control group, whereas pretreatment with 100 or 500 μg/ml CSE significantly inhibited the decrease induced by H_2O_2 stress. These results confirm that CSE upregulates Nrf2 expression in the nucleus, which may have caused the observed induction of GSH expression in this study.

In this study, we demonstrated that CSE protected human keratinocytes from oxidative stress. This effect may stem primarily from its antioxidant activities such as its repression of ROS generation and up-regulation of SOD, CAT, and GSH expression (which follow the induction of Nrf2 expression). The CSE used in this study contained 47.06 mg/g fatty acids, which were found in gas chromatography analyses to be mostly of medium chain length ($C_{16–18}$). The major fatty acids were linoleic acid and linolenic acid (accounting for 30.34 and 38.05% of fatty acids, respectively; table 1), which have been reported in previous studies to have antioxidative and therapeutic effects in various skin diseases [23–26]. Furthermore, they have been reported to inhibit UVB- and H_2O_2-induced stress in fibroblasts [27]. Thus, linoleic and linolenic acid in CSE may contribute partly to the observed protection of keratinocytes from H_2O_2-induced stress in this study.

In summary, CSE protected against H_2O_2-induced oxidative stress by inhibiting ROS production, upregulating oxidative defense enzyme expression, and increasing nuclear Nrf2 levels. These results suggest that CS may be a useful candidate for protecting skin cells from oxidative damage.

Acknowledgement

This work was carried out with the support of the Cooperative Research Program for Agriculture Science and Technology Development (PJ0074792011), Rural Development Administration, Republic of Korea.

References

1 Klaunig JE, Kamendulis LM: The role of oxidative stress in carcinogenesis. Annu Rev Pharmacol Toxicol 2004;44:239–267.
2 Jain A, Rieger I, Rohr M, Schrader A: Antioxidant efficacy on human skin in vivo investigated by UVA-induced chemiluminescence decay analysis via induced chemiluminescence of human skin. Skin Pharmacol Physiol 2010;23:266–272.
3 Jeon HY, Kim JK, Seo DB, Cho SY, Lee SJ: Beneficial effect of dietary epigallocatechin-3-gallate on skin via enhancement of antioxidant capacity in both blood and skin. Skin Pharmacol Physiol 2010;23:283–289.
4 Nevin KG, Rajamohan T: Effect of topical application of virgin coconut oil on skin components and antioxidant status during dermal wound healing in young rats. Skin Pharmacol Physiol 2010;23:290–297.
5 Kobayashi M, Yamamoto M: Molecular mechanisms activating the nrf2-keap1 pathway of antioxidant gene regulation. Antioxid Redox Sign 2005;7:385–394.
6 Lee JM, Johnson JA: An important role of Nrf2-ARE pathway in the cellular defense mechanism. J Biochem Mol Biol 2004;37:139–143.
7 Schafer M, Dutsch S, auf dem Keller U, Navid F, Schwarz A, Johnson DA, Johnson JA, Werner S: Nrf2 establishes a glutathione-mediated gradient of UVB cytoprotection in the epidermis. Genes Dev 2010;24:1045–1058.
8 Motohashi H, Yamamoto M: Nrf2-Keap1 defines a physiologically important stress response mechanism. Trends Mol Med 2004;10:549–557.
9 Kimura S, Warabi E, Yanagawa T, Ma D, Itoh K, Ishii Y, Kawachi Y, Ishii T: Essential role of Nrf2 in keratinocyte protection from UVA by quercetin. Biochem Biophys Res Commun 2009;387:109–114.
10 Saw CL, Huang MT, Liu Y, Khor TO, Conney AH, Kong AN: Impact of Nrf2 on UVB-induced skin inflammation/photoprotection and photoprotective effect of sulforaphane. Mol Carcinog 2011;50:479–486.
11 Hashim MS, Lincy S, Remya V, Teena M, Anila L: Effect of polyphenolic compounds from *Coriandrum sativum* on H_2O_2-induced oxidative stress in human lymphocytes. Food Chem 2005;92:653–660.
12 Chithra V, Leelamma S: *Coriandrum sativum* effect on lipid metabolism in 1,2-dimethyl hydrazine induced colon cancer. J Ethnopharmacol 2000;71:457–463.
13 Reuter J, Huyke C, Casetti F, Theek C, Frank U, Augustin M, Schempp C: Anti-inflammatory potential of a lipolotion containing coriander oil in the ultraviolet erythema test. J Dtsch Dermatol Ges 2008;6:847–851.
14 Chithra V, Leelamma S: *Coriandrum sativum* changes the levels of lipid peroxides and activity of antioxidant enzymes in experimental animals. Indian J Biochem Biophys 1999;36:59–61.
15 Zhou ZF, Chen LY, Shen M, Ma AD, Yang XM, Zou F: Analysis of the essential oils of *Coriandrum sativum* using GC-MS coupled with chemometric resolution methods. Chem Pharm Bull (Tokyo) 2011;59:28–34.
16 Neffati M, Marzouk B: Changes in essential oil and fatty acid composition in coriander (*Coriandrum sativum* L.) leaves under saline conditions. Ind Crop Prod 2008;28:137–142 (erratum published in Ind Crop Prod 2009;29:657–657).
17 Bajpai M, Mishra A, Prakash D: Antioxidant and free radical scavenging activities of some leafy vegetables. Int J Food Sci Nutr 2005;56:473–481.
18 Kim HG, Ju MS, Shim JS, Kim MC, Lee SH, Huh Y, Kim SY, Oh MS: Mulberry fruit protects dopaminergic neurons in toxin-induced Parkinson's disease models. Br J Nutr 2010;104:8–16.
19 Shim JS, Kim HG, Ju MS, Choi JG, Jeong SY, Oh MS: Effects of the hook of *Uncaria rhynchophylla* on neurotoxicity in the 6-hydroxydopamine model of Parkinson's disease. J Ethnopharmacol 2009;126:361–365.
20 Emonet-Piccardi N, Richard MJ, Ravanat JL, Signorini N, Cadet J, Beani JC: Protective effects of antioxidants against UVA-induced DNA damage in human skin fibroblasts in culture. Free Radic Res 1998;29:307–313.
21 Bertling CJ, Lin F, Girotti AW: Role of hydrogen peroxide in the cytotoxic effects of UVA/B radiation on mammalian cells. Photochem Photobiol 1996;64:137–142.
22 Takebe G, Yarimizu J, Saito Y, Hayashi T, Nakamura H, Yodoi J, Nagasawa S, Takahashi K: A comparative study on the hydroperoxide and thiol specificity of the glutathione peroxidase family and selenoprotein P. J Biol Chem 2002;277:41254–41258.
23 Yen CH, Dai YS, Yang YH, Wang LC, Lee JH, Chiang BL: Linoleic acid metabolite levels and transepidermal water loss in children with atopic dermatitis. Ann Allergy Asthma Immunol 2008;100:66–73.
24 Ando H, Ryu A, Hashimoto A, Oka M, Ichihashi M: Linoleic acid and alpha-linolenic acid lightens ultraviolet-induced hyperpigmentation of the skin. Arch Dermatol Res 1998;290:375–381.
25 Decker EA: The role of phenolics, conjugated linoleic acid, carnosine, and pyrroloquinoline quinone as nonessential dietary antioxidants. Nutr Rev 1995;53:49–58.
26 Punnonen K, Jansen CT, Puntala A, Ahotupa M: Effects of in vitro UVA irradiation and PUVA treatment on membrane fatty acids and activities of antioxidant enzymes in human keratinocytes. J Invest Dermatol 1991;96:255–259.
27 Bonina F, Puglia C, Avogadro M, Baranelli E, Cravotto G: The topical protective effect of soybean-germ oil against UVB-induced cutaneous erythema: an in vivo evaluation. Arch Pharm (Weinheim) 2005;338:598–601.